Check for updates

Increased water presence in phospholipid fluid bilayers upon addition of lysolipids†

Fernanda Alvarado Galindo, [iD] *[ab] Joachim Venzmer,[c] Najet Mahmoudi, [iD] [d] Michael Gradzielski [iD] [b] and Ingo Hoffmann [iD] *[a]

In spite of the numerous studies dealing with the interaction between lipid membranes and surfactants at subsolubilizing membrane concentrations, quantifying detailed bilayer structure, as for instance pore formation, on phospholipid bilayers upon addition of single chain lipids continues to be a challenge. Herein, we analyze the effects of lysophosphatidylcholine (18 : 1 LPC or lysolipid) on soybean phosphatidylcholine (SPC) extruded liposomes, where vesicles containing additional LPC exhibit approximately a 10% reduction in size as indicated by dynamic light scattering experiments. Most importantly, we benefit from the non-perturbing nature of small-angle neutron scattering (SANS) measurements to determine the degree of water incorporation presumably through the surfactant stabilized pores along the fluid bilayers. Model-free analysis of SANS curves reveals that the membrane part of the pure SPC vesicles contain 3.3% v of water. As the lysolipid is added to the dispersion, the volume fraction of water counted into the lipid membrane ($\phi_{D_2O}^{lipo}$) increases to 15–20%. Finally, assuming $\phi_{D_2O}^{lipo}$ to be equivalent to the volume fraction of pores within the bilayers we estimate the pore size and density.

1 Introduction

Phospholipids (PLs) self-assemble when dispersed in an aqueous solution and form closed concentric bilayers commonly known as liposomes. Thanks to particle morphology and ability to encapsulate hydrophobic, hydrophilic, or amphiphilic molecules, PL liposomes have become an established delivery form in pharmacology and cosmetics.[1–3] The enveloped active ingredients can be released under pre-stated conditions,[4] for which membrane properties become an important aspect for industrial formulations where a balance between excellent barrier properties and extremely permeable liposomes has to be met.[5]

Membrane permeation can be altered by external factors (temperature, pH, light, *etc.*) or by lipid composition. For the latter, it is known that adding surfactants to liposomal dispersions disrupts the membrane since they alter the bilayer organization by inducing curvature stress.

[a] Institut Max von Laue-Paul Langevin (ILL), F-38042 Grenoble Cedex 9, France. E-mail: hoffmann@ill.fr

[b] Stranski-Laboratorium für Physikalische und Theoretische Chemie, Institut für Chemie, Technische Universität Berlin, Straße des 17. Juni 124, Sekr. TC 7, D-10623 Berlin, Germany

[c] Evonik Operations GmbH, Essen, Germany

[d] Rutherford Appleton Laboratory, ISIS facility, Science and Technology Facilities Council, Harwell Science & Innovation Campus, OX11 0QX, Didcot, UK

† Electronic supplementary information (ESI) available. See DOI: https://doi.org/10.1039/d4sm01211a

Thus, surfactant-membrane interactions have been an intensive topic of study over the years.[6,7] Surfactants partition into the lipid bilayer from the bulk solution,[8] starting from concentrations below their critical micellar concentration (CMC) (4–8.3 μM for lysolipids[9]). Subsequent alterations to the bilayer depend on the properties of the amphiphile and the speed of flip-flop motion between the inner and outer monolayers. This motion is classified into "slow" and "fast" based on the exchange rate and time needed for membrane solubilization.[10] For example, lysophosphatidylcholines (LPCs) are considered "slow" surfactants as their bulky headgroup inhibits fast exchange between the monolayers.[11] SDS (another "slow" agent) has a flip-flop rate of minutes to hours at room temperature, whereas "fast" amphiphiles have a flipping rate on the order of 0.5 s.[12]

When surfactant molecules are present in both the inner and outer monolayers, they may cause a discontinuity in the bilayer, forming transient holes (or pores) along the liposome surface.[13] Such an event is possible if the amphiphiles cover the pore edges and prevent exposure of the hydrophobic bilayer core to the aqueous environment. Pore formation has been evidenced by results from optical microscopy,[14,15] kinetic measurements[16] and molecular dynamics (MD) simulations.[12]

Consequently, the barrier properties of the bilayer are reduced, resulting in increased membrane permeability upon addition of a surfactant, as observed through fluorescence,[4,17] glucose,[18] and ion exchange[19,20] studies. The increased permeability observed through release assays has also been correlated

to a decrease in the bending modulus of the membrane.[21–24] Thus, it is clear that fluid PL bilayers will suffer gradual structural changes in the presence of a lysolipid before suffering disintegration under formation of mixed micelles (starting at 30% mol lysolipid, although an exact number depends on the precise molecular composition[20,25]).

Here, we are interested in the changes on soybean phosphatidylcholine (SPC) fluid bilayers when prepared with LPC at sub-solubilizing concentrations. Our study involves systematically introducing LPC to a high-quality SPC mixture ($\geq$94% PC) containing no more than 3% LPC. First, we employ light and small-angle neutron scattering (SANS) as non-perturbing techniques that capture the changes in particle size and bilayer morphology, respectively. In SANS experiments, we benefit from the difference in scattering length density between hydrogen and deuterium to examine our systems and estimate the volume fraction of water incorporated into the liposome membrane by model-free analysis of the curves, providing valuable information about the incorporation of water in the membrane at different LPC concentrations.

2 Materials and methods

2.1 Materials

Soybean phosphatidylcholine (SPC), Lipoid S100, at >94% phosphatidylcholine (PC) was kindly supplied by Lipoid, France. We assume a scattering length density of 0.32×10^{10} cm^{-2} for SPC, based on an average composition $C_{42}H_{80}NO_8P$ (Fig. 1) and a density of 1.01 g cm^{-3}.[26] For 1-oleoyl-2-hydroxy-sn-glycero-3-phosphocholine (18:1 LysoPC, Avanti, c) at PC > 99%, we assume a SLD of 0.39×10^{10} cm^{-2} and a density of 1.08 g mL^{-1}. LPC density was calculated assuming a lysolipid volume of ~800 Å^3, considering reported volumes of DOPC and PC headgroups of ~1300 Å^3 and ~ 300 Å^3, respectively.[27] LPC and deuterium oxide (D$_2$O, 99.9%) were purchased from Sigma Aldrich, France. Lipids were used as received.

2.2 Preparation of phospholipid liposomes

Liposomes containing SPC and SPC-lysophosphatidylcholine (LPC) were obtained by mixing the lipids in aqueous solution with a magnetic stirrer and extruding the lipid dispersion at least 21 times through a polycarbonate membrane with a mini extruder (Avanti Polar Lipids, United States) at room temperature (RT). SPC content was fixed at 0.5% w and either 0.01% w, 0.02% w, or 0.05% w LPC was added to the mixture. Samples for small-angle neutron scattering (SANS) experiments were dispersed in heavy water (D$_2$O) and extruded for 21 times with a

Fig. 1 Structures of (A) SPC based on an average composition $C_{42}H_{80}NO_8P$ and (B) 18:1 LPC.

200 nm and a 100 nm membrane, each (total of 42 times), as to reduce particle size to the accessible q-range in SANS.

2.3 Light scattering

Dynamic (DLS) and static light scattering (SLS) were realized using an ALV/CGS-3 Compact Goniometer system with a HeNe Laser (wavelength λ = 632.8 nm) at a temperature T = 25 °C. Intensity autocorrelation functions $g^{(2)}$ were recorded using an ALV7004/FAST real time multiple tau digital correlator. The scattering angle was set to 90°. All measurements were repeated 5 times and averaged with an acquisition time of 30 s for each individual measurement. SLS experiments were performed at different angles to access a q-range of 0.0009 1 Å^{-1} < q < 0.0024 1 Å^{-1}, where q is the magnitude of the scattering vector q = $(4\pi n_s/\lambda)\sin(\theta/2)$ and n_s the refractive index of the solvent. Forward scattering (I_0) can be calculated using the Guinier approximation (eqn (SI 1), ESI†), whereas the mass-average molecular weight is obtained by inputting I_0 in eqn (SI 2), ESI.†

2.4 Small-angle neutron scattering (SANS)

SANS experiments were carried out on the Sans2d diffractometer at the ISIS Pulsed Neutron Source (STFC Rutherford Appleton Laboratory, Didcot, U.K.). Samples were loaded in 2 mm cuvettes and placed in the sample holder under temperature control of 25 °C. A q-range of 0.0023–0.99 1 Å^{-1} was accessible utilizing an incident wavelength range of 1.75–14.4 Å and merging data recorded on two detectors positioned 8 m and 4 m away from the sample. Data reduction including correction for background, empty cell scattering, transmissions, detector efficiency, data radial averaging and transformation to absolute intensities was done using the software Mantid.[28] To convert to absolute scale a solid blend of hydrogenated and perdeuterated polystyrene sample was used.

For a system with two components and sharp interfaces the scattering invariant

$$Q_{inv} = \int_0^\infty q^2 I(q)\mathrm{d}q \qquad (1)$$

is directly linked to the volume fractions of the components

$$Q_{inv} = 2\pi^2 \phi_1 \phi_2 \Delta SLD^2, \qquad (2)$$

where ϕ_i is the volume fraction of component i and ΔSLD is the scattering length density difference between the two components. Eqn (2) is valid regardless of the shape and structure of the two phases. Q_{inv} was obtained from the integration of the SANS curves and summing the contributions from the Guinier and Porod regions as detailed in the ESI.† Here, we treat our dispersions as a two component system, made of liposomes composed of double and single chain phospholipids (SPC and LPC) and solvent. At concentrations of the LPC below bilayer solubilization, all lipids are assumed to reside in the liposome phase and a fraction of water can penetrate into the lipid bilayer while the remainder forms the solvent phase, so that the volume fraction of the liposomes is given by

$$\phi_{lipo} = \phi_{SPC} + \phi_{LPC} + \beta\phi_{wat} \qquad (3)$$

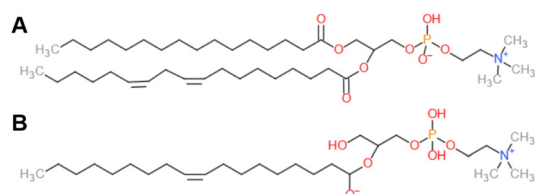and the volume fraction of the solvent phase is given by

$$\phi_{solvent} = (1 - \beta)\phi_{wat}, \qquad (4)$$

where β is the fraction of water contained in the liposome membranes. As a consequence, the SLD of the liposomes reads

$$SLD_{lipo} = \left[\frac{1}{\phi_{lipo}}\right][\phi_{SPC}SLD_{SPC} + \phi_{LPC}SLD_{LPC} + \beta\phi_{wat}SLD_{wat}],$$

$$(5)$$

where the solvent SLD will be that of heavy water (SLD_{wat}).

If no solvent were to penetrate the liposome phase, β in eqn (3)–(5) would equal zero and the theoretical invariant (Q_{inv}^{theo}) was calculated as such.[29] However, if water was to penetrate the membrane and $\beta > 0$, then for small β, ϕ_{lipo} increases linearly, while ΔSLD_{lipo} decreases linearly and as the latter enters eqn (2) quadratically, the overall value of Q_{inv} decreases. See Fig. SI3 and eqn (SI 12) (ESI†) for the graphic and analytical relation between Q_{inv} and β.

3 Results and discussion

3.1 Light scattering

DLS measurements were performed on SPC and SPC/LPC liposomes extruded with a 100 nm membrane. The hydrodynamic radius (R_h) was calculated from the Stokes–Einstein relation with the relaxation rate obtained from cumulant analysis of the correlation curves.

Comparing the R_h vs. LPC content in Fig. 2, we observe that samples with added lysolipid have a smaller particle size as the R_h of SPC liposomes is $\sim$60 nm and reduces to $\sim$55 nm for the three studied SPC : LPC ratios (98 : 2, 96 : 4, 91 : 9). In addition, the polydispersity index (PDI) increases from 0.03 to 0.1, so the systems have a low, yet increasing, polydispersity (Table 1). The likely explanation for the reduction of the size is the reduction
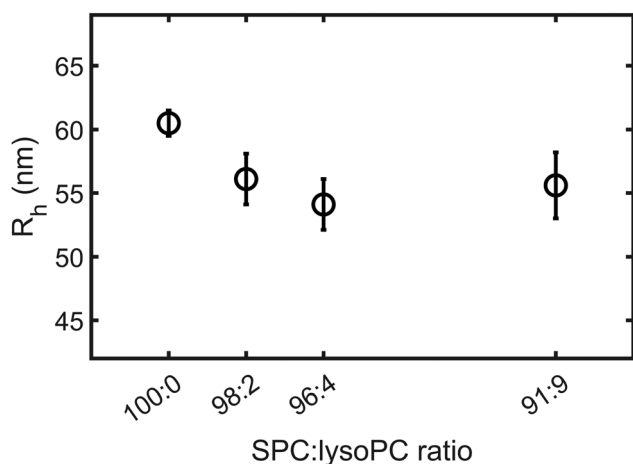
of the membrane rigidity, as addition of LPC has been reported to reduce the bending modulus by a factor 4.[21] The softer membranes are then more easily deformed during extrusion, leading to formation of smaller vesicles. For a comparison, it might be noted that subsequent addition of lysolipids leads to almost no size change for liposomes formed by the rehydration or sonication processes.[30]

Results from SLS experiments summarized in Table 1 support the reduction in particle size observed by DLS since we observe a decrease in radius of gyration (R_g) that is well correlated to a reduction in the vesicular molecular weight (MW_{lipo}), estimated using eqn (SI 2) (ESI†). MW_{lipo} is compared to the molecular weight of unilamellar vesicles (ULV) to estimate the lamellarity (N_{bi}) in our systems assuming a double bilayer with a spacing between the bilayers of 2 nm.[32]

The molecular weight of ULVs was calculated from R_h and using a lipid density of 1.01 g cm^{-3}.[26] Since the bilayer thickness is known to decrease in the presence of lysolipids,[33] literature values were used to estimate N_{bi}.

As a result, we find a value of $N_{bi} \sim 1.6$ for pure SPC liposomes that decreases down to $N_{bi} \sim 1.5$ with added LPC. It is conceivable for bilamellar and unilamellar vesicles (ULV) to coexist in the extruded dispersion, as vesicles with more than one bilayer are known to persist in spite of the extrusion process.[34] To increase the abundance of ULVs without modifying the chemical composition of the bilayer, or of the aqueous environment, shearing with a smaller membrane pore size is required.[34]

A reduction of N_{bi} at higher lysolipid ratios is in line with the idea that softer membranes are more easily deformed by extrusion, making it easier to disrupt the multillamelarity of the vesicles. Moreover, we calculated the shape factor defined as R_g/R_h which provides an indication of particle morphology. A value of 1, close to our values is characteristic of hollow spheres, i.e. confirming that the two bilayers are close together.[35]

3.2 Small-angle neutron scattering

To elucidate the changes in liposome structure and composition, we study LPC containing liposomes with SANS. The difference of scattering length density between deuterium and hydrogen atoms allows the study of structural changes. In particular, we exploit the information provided by the scattering invariant (Q_{inv}) (eqn (1)) from our SPC–LPC assemblies.

Fig. 2 Evolution of the hydrodynamic radius (R_h) of extruded SPC liposomes (using a 100 nm pore size membrane) upon addition of lysophosphatidylcholine (18 : 1, LPC) to the lipid formulation. Decrease of R_h with increasing LPC content is presumably due to reduced membrane bending moduli. R_h was determined from DLS measurements at $\theta = 90°$ at 25 °C.

Table 1 Particle sizes and shape factor obtained from dynamic (DLS) and static light scattering (SLS) experiments for extruded liposomes with different SPC : LPC ratios. Apparent vesicular molecular weight (MW_{lipo}) was estimated from the forward scattering obtained by SLS. The number of bilayers or lamellarity (N_{bi}) was assessed by comparing MW_{lipo} with that of a unilamellar vesicle (ULV), calculated from the experimental R_h and bilayer thickness (δ) values reported in the literature.[31] Lipid density was assumed to be 1.01 g cm^{-3}[26] whereas bilayer spacing was obtained from the SANS curves presented in Fig. SI 5a (ESI)

SPC : LPC	R_h (nm)	Shape factor (R_g/R_h)	$MW_{lipo} \times 10^8$ (g mol^{-1})	δ (nm)	$\delta_{solvent}$ (nm)	N_{bi}
100 : 0	60.5 ± 1.1	1.09 ± 0.09	1.850	3.9	3.2	1.65
98 : 2	56.1 ± 2.3	1.08 ± 0.14	1.424	3.8	3.4	1.53
96 : 4	54.1 ± 2.6	1.06 ± 0.15	1.265	3.7	3.0	1.50
91 : 9	55.6 ± 2.9	1.06 ± 0.16	1.322	3.6	3.0	1.50

The SANS curves presented in Fig. 3 follow mostly a $q^{-2.3}$ decay in the mid-q region (0.001 1 Å^{-1} < q < 0.005 1 Å^{-1}) at the studied SPC : LPC ratios. A power-law of -2 is characteristic of flat surfaces and consequently, would be expected for large unilamellar vesicles where the surface properties dominate. For smaller sized vesicles and for increasing number of shells, the multilamellar vesicles exhibit compact volume properties (spheres) and the exponent of the power-law increases.[36] The multilamellarity of the vesicles is further corroborated by the weak peak at about 0.1 1 Å^{-1}. Therefore, we decided to fit the curves as a weighted sum of uni- and bilamellar vesicles according to the results for N_{bi} from light scattering (see Table 1). The relative standard deviation for modelling was set to 0.3 for the vesicle radius and bilayer thickness. The complete set of parameters employed is shown in Table SI 4 (ESI†).

In qualitative agreement with the results from light scattering, it can be seen that the shallow peak at 0.1 1 Å^{-1} becomes weaker as more LPC is added, which means that the vesicles become more unilamellar and the form factor minimum at about 0.006 1 Å^{-1} becomes more smeared out, which means that the vesicles become more polydisperse and/or softer.[37] From light scattering and SANS investigations, it is evident that LPC promotes the presence of ULVs rather than multilamellar vesicles (MLVs). If LPC softens the membrane, the bilayers may be easily deformed by the extrusion process and this would lead to reduced lamellarity. Additionally, LPC is known to alter the bilayer structure, allowing an increase in area per-lipid in the outer monolayer and a compression of the inner one. This structural modification promotes increased curvature, which could also disfavor the formation of MLVs.[38]

3.3 Presence of water in liposome bilayers using the scattering invariant analysis

The scattering invariant (Q_{inv}, eqn (1)) is an integral parameter independent from the structure, interparticle interactions, or the distribution of domains, and is a constant directly proportional to the square of the contrast between two domains of different, constant SLD in the system (eqn (2)), where one typically makes the assumption that such a simplified description of a scattering system can be done, as in our case for the aqueous domain and the part constituting the bilayers. More importantly, Q_{inv} depends on the volume fraction of the lipids (ϕ_{lipo}) and such a relation is important in that it will change if the bilayer swells.

As a consequence, the contrast between the components (ΔSLD) will be modified since the scattering length density of the self-assemblies will have an additional contribution, that is, of the incorporated water (eqn (5)) and the experimental invariant decreases upon water incorporation as described in Section 2.4.

To analyze how the experimental Q_{inv} deviates from the estimated theoretical value, Q_{inv}^{theo} is calculated by mass balance, assuming water does not penetrate the membrane. This corresponds to $\beta = 0$ with eqn (3)–(5) and Q_{inv}^{theo} was calculated as such. The experimental invariants were obtained from SANS curves as described by eqn (1) and are presented in Fig. 4. On the one hand, we observe that Q_{inv}^{theo} grows with addition of lysolipid to the system due to the increase of the lipid volume fraction. On the other hand, it is apparent that Q_{inv} drops with small amounts of added LPC and grows again at higher LPC contents but remains smaller than Q_{inv}^{theo} by a relatively constant offset, while the experimental and theoretical values show good agreement for SPC without added LPC. This indicates the presence of small amounts of water in the SPC bilayers. See Table SI 3 (ESI†) for detailed results of the numerical and extrapolated values taken into account for derivation of Q_{inv}.

One hypothetical possibility for the lower Q_{inv} values would be a dissolution of lipids into the solvent, but given the molecular architecture of the lipids and low CMC of the lysolipid (between 4–8.3 μM[9]) this is a very unlikely scenario. Here, we work above
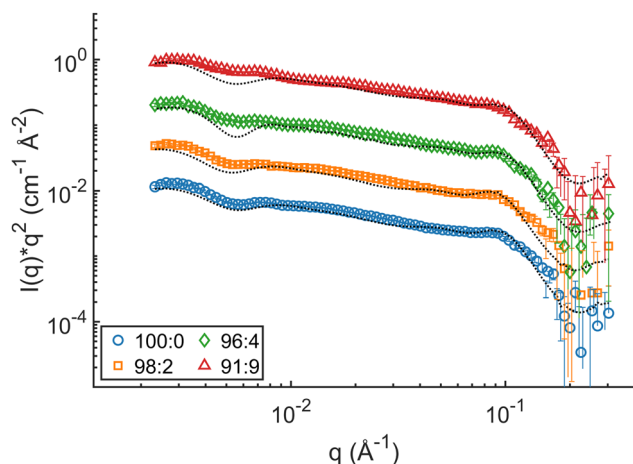

Fig. 3 Kratky plots ($I(q)q^2$ *vs. q*) of SANS data of liposomes extruded with a 100 nm pore size membrane at different SPC : LPC ratios. At increasing LPC content, liposomes become more unilamellar and more polydisperse. Dashed lines correspond to data fits using a combination of unilamellar and multilamellar vesicle form factor (see Table SI 4, ESI† for a summary of the fitting parameters). Curves are shifted by a factor 1, 5, 20 and 100 for easier visualization.
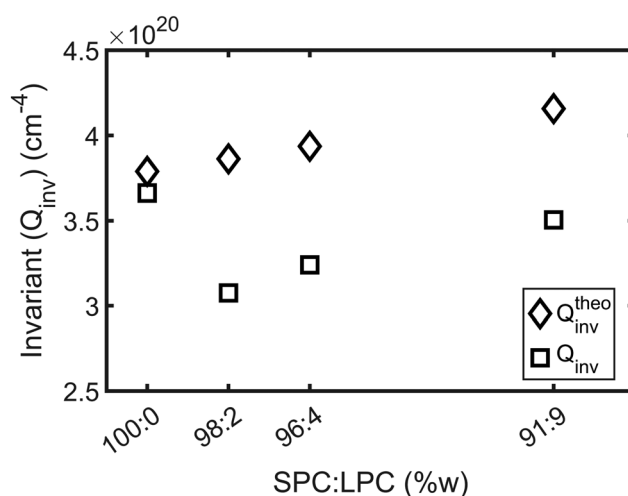

Fig. 4 Comparison of the theoretical (Q_{inv}^{theo}) and experimental (Q_{inv}) scattering invariants obtained from the model-free analysis of SPC : LPC liposomes SANS curves. Q_{inv} systematically fall short from Q_{inv}^{theo}, derived from mass balance from parameters detailed in Table SI 2 (ESI†) at all the studied SPC : LPC ratios.

the cmc from the lowest LPC ratio, where the LPC concentration is 191 μM. Therefore, the logical answer is that the lower Q_{inv} values result from an increased water presence within the lipid membrane, potentially due to the presence of surfactant stabilized pores.[14,16,39,40] Consequently, this would increase ϕ_{lipo} and decrease ΔSLD as previously explained.

To quantify the fraction of water incorporated into the lipid phase (β), we solved eqn (3)–(5) (see eqn (SI 13) (ESI†)) to estimate the volume fraction of solvent that needs to be incorporated in the membrane to explain the deviations in Q_{inv}. Thereafter we calculated the fraction of water contained in the lipid part of the system ($\phi_{D_2O}^{lipo} = \beta\phi_{D_2O}/\phi_{lipo}$) and show our results in Fig. 5.

Based on the calculated values, the SPC sample with no added lysolipid is only slightly hydrated as $\phi_{D_2O}^{lipo}$ is approximately 3%. However, the fraction of incorporated water increases strongly upon the addition of LPC as $\phi_{D_2O}^{lipo}$ rises to 20% at a 98:2 SPC:LPC ratio and slightly decreases to 15% upon further addition of the lysolipid.

The fact that $\phi_{D_2O}^{lipo}$ does not increase further when increasing the SPC:LPC ratio past 98:2 might indicate that extra LPC forms small micelles, which would be essentially invisible next to the vesicles in the SANS curves[41] and they are not accounted for in the proposed pore model since they would have no water. Thus, if the additional LPC forms dry micelles, the water volume within the membrane pores should remain constant. Given the relation $\phi_{D_2O}^{lipo} = \beta\phi_{D_2O}/\phi_{lipo}$, an increase in lipid concentration and constant amount of incorporated water would decrease $\phi_{D_2O}^{lipo}$, which is the trend observed in Fig. 5.
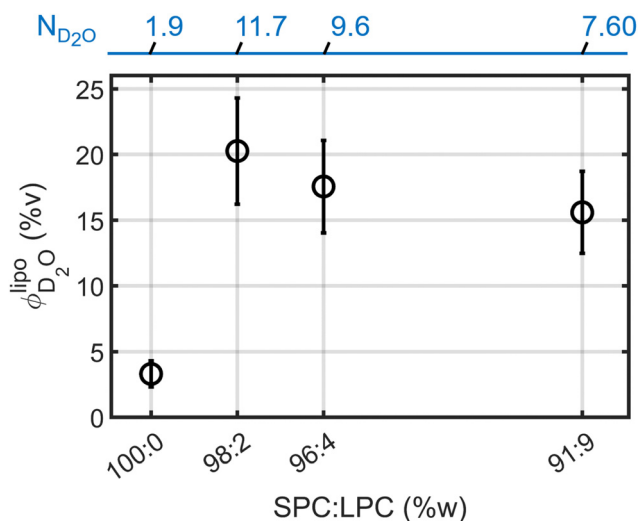

Fig. 5 Graphic representation of the calculated volume fractions of D_2O incorporated to the SPC liposomes from model-free analysis of SANS curves. The presence of water in the membrane increases upon addition of a lysophosphatidylcholine (18:1, LPC) of similar chain-length to that of the SPC. Assuming deviations of the scattering invariant (Q_{inv}) to the values calculated by mass balance, the amount of water within the membrane core responsible for said deviations was estimated with eqn (SI 13) (ESI†). On the top, the hydration number N_{D_2O} (molecules of water per molecule of lipid) estimated from $\phi_{D_2O}^{lipo}$.

This would also explain the consistent differences between Q_{inv} and Q_{inv}^{theo} observed in Fig. 4.

It is also possible that this increased water content is due to simple diffusion. According to Seu et al. the removal of an alkyl chain by addition of LPC should reduce van der Waals interactions and make the membrane more fluid.[42] This could be correlated to the increased membrane permeability deduced also by coarse grained simulations. However, it remains unclear whether these changes are due to modifications in the area-per-lipid or due to the appearance of transient pores.[43]

What is certain is that the architecture of LPC plays an important role in the bilayer properties. For instance, a similar surfactant like monopalmitoyl-glycerol, single C_{16} alkyl chain with a glycerol backbone but without the bulky PC headgroup, was not observed to increase bilayer permeability unlike its C_{16} lysolipid counterpart.[44] It is with the presence of lysolipid that readjustments of area-per-lipid take place to adapt to the local curvature.[38,45]

To corroborate if the values resulting from the invariant analysis are feasible, we estimated the hydration number N_{D_2O} (water molecules per lipid molecule) from $\phi_{D_2O}^{lipo}$. Assuming that all the lipids partake in the self-assembly, we calculated the number of surfactant molecules in the dispersion from the lipid concentrations and molecular weights following eqn (SI 14) (ESI†), attributing the corresponding number of water molecules per lipid from $\phi_{D_2O}^{lipo}$.

For liposomes with added LPCs, N_{D_2O} ranges from 7.6 to 11.7 (Fig. 5). This degree of hydration is comparable to the N_{H_2O} reported for PC dispersions with lipids of similar chain-length ($N_{H_2O} = 8–13$).[46–48] However, it is likely that our N_{D_2O} falls short for a fully hydrated lipid bilayer since the hydrated lipid headgroups are mostly invisible for SANS, given that they are not really incorporated into what geometrically is to be considered as the bilayer and that concerns hydration water molecules on the surface of the bilayers pointing to the aqueous part of the system. This then leads one to wonder where exactly this large amount of extra water seen upon addition of LPC is located within the bilayer. For sure this shows that here a structural change of the bilayer must have occurred. One logical option one could think of would be the formation of pores/holes within the bilayer, which are stabilized by the LPC.

At low concentrations, the lysolipid should be incorporated into the lipid bilayer and the inverted cone structure of LPC would promote positive curvature of the membrane.[33,38] Further addition of surfactant should create LPC enriched regions with a localized high curvature. This structural feature should foster the formation of pores or domains of high curvature to prevent exposure of the hydrophobic bilayer core to water. Past a critical SPC:LPC ratio, the membrane will no longer be able to accommodate more surfactant and beyond this critical point, further LPC will assemble in form of micelles.[40] Unfortunately, we would not be able to corroborate the formation of micelles with the employed contrast, since the micelle scattering signal would be effectively shadowed by that of the vesicles (Fig. SI 6, ESI†).

Here we observe increased water presence in the liposomes and suggest which structural changes may explain this. Further experiments such as permeability studies, could shed some light on the matter, keeping in mind that we presume to be in the presence of small pores. Therefore, size of the hydrophilic solute and liposome preparation method would be relevant for comparison of the results.

3.4 Estimating pore size and density

While our results do not allow us to differentiate between transient pores or diffusion, we can nevertheless estimate the size and density of pores if the added water in the membrane was due to pores based on some simple geometrical considerations. Assuming that LPC promotes the formation of transient pores, we can estimate a pore radius (R_{pores}) and area density (ρ_{pore}) making the following assumptions: (1) the LPC stabilizes the pores and therefore the headgroup area of the LPC forms the pore walls. (2) We assume that all of the LPC is found in the pore walls. (3) The water in the membranes $\phi_{D_2O}^{lipo}$ corresponds to the pore volume. With these assumptions, we obtain a volume to area ratio and, assuming a specific shape, we can calculate a pore size, which can be used to calculate a pore area density. For the sake of simplicity, we assume a simple cylindrical shape of the pores (see Fig. 6(A)) so that $V_{cylinder}/A_{cylinder} = R_{cylinder}/2$, which is obviously an oversimplification but should still yield a reasonable ballpark number.

Looking at Fig. 5 it is clear that our assumptions only hold (at most) up to an SPC:LPC ratio of 98:2 as further addition of LPC does not lead to an increase of water in the membranes and we simply take the slope between the sample without LPC and the sample with SPC:LPC 98:2 to obtain a volume ratio $V_{pores}/V_{LPC} = 10.8$ (see Fig. SI 7, ESI†). With the known molecular weight ($MW_{LPC}= 521.67$ g mol^{-1}), specific volume ($\hat{V}_{LPC} =$

Fig. 6 Schematic representation of surfactant stabilized pores along the lipid membrane of a liposome used to estimate a pore density. In reality, it is likely that the pore walls are simply LPC enriched and that they are much smaller than what the scheme suggests, so that the water would scatter as part of the liposome and not of the bulk solution. The LPC-belt stabilizing the pore is represented in green assuming (A) a cylindrical or (B) torus geometrical shape of the belt. Water penetrates the membrane through the pore, thus the volume fraction of water in the liposome, $\phi_{D_2O}^{lipo}$ increases.

Table 2 Percentage of the vesicle area covered by pores ($R^2\rho_{pore}$), calculated with the pore densities (ρ_{pore}) of SPC–LPC liposomes obtained from the distance between pores assuming $\rho_{pores} = 1/L^2$. The area covered by pores in a given liposome increases at higher LPC mass ratios. Considering a small unilamellar vesicle (SUV) with the R_h reported in Table 1, its resulting surface area is used to calculate the number of pores per vesicle (N_{pores}/N_{SUV}). The two limits for the reported parameters are derived from the assumption that the LPC belt stabilizing the pore has a cylindrical or torus structure (indicated by [†])

SPC:LPC	$R^2\rho_{pore}$ (%)	N_{pores}/N_{SUV}	$R^{2(†)}\rho_{pore}^{†}$ (%)	$N_{pores}^{†}/N_{SUV}$
100:0	1.21	0.79	1.19	1.19
98:2	7.42	4.13	7.27	6.24
96:4	6.43	3.33	6.30	5.03
91:9	5.71	3.13	5.59	4.73

0.9246 mL g^{-1} assuming a V_{LPC} of 800 Å^3 based on reported volumes for DOPC and PC headgroups[27]) and headgroup area of LPC ($A_{LPC} \simeq 70$ Å^2(ref. 23 and 49)), we can convert the volume V_{LPC}^{lipo} to an area and with that calculate a pore radius according to
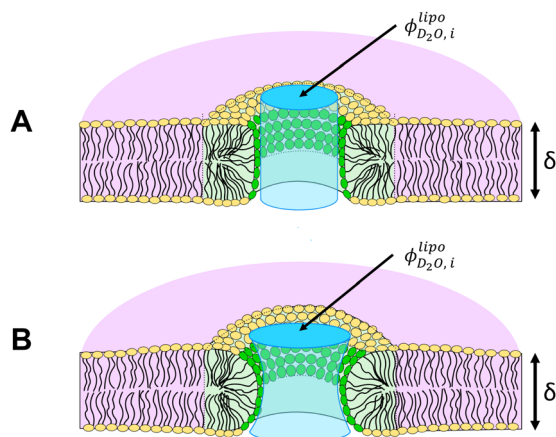
$$R_{pores} = 2\frac{V_{pores}}{A_{LPC}^{pores}} = 2\frac{V_{pores}}{V_{LPC}^{lipo}}\frac{MW_{LPC}\hat{V}_{LPC}}{N_A A_{LPC}} \quad (6)$$

The values obtained for R_{pores} seem rather large and if there were pores with a size on the order of 20 nm it should be possible to detect them using electron microscopy. However, to the best of our knowledge the existence of such pores has not been reported before. In addition, such large pores would have sharp boundaries and the water contained in them would scatter as part of the bulk solution and not the liposome. Then, the variation in the scattering invariant should be explained differently. So, we have to assume that there either are no pores or the pores are significantly smaller than suggested by our calculations, a few nm at most.

Looking at eqn (6) the pore radius would decrease if A_{LPC}^{pores} would increase and we could relax assumption 1, and instead of assuming that the pore walls are made of LPC exclusively as shown in Fig. 6, we could simply assume that LPC is enriched in the pore walls. Pores on the order of 2 nm would be very difficult to detect by electron microscopy. Such pores would result from eqn (6) if we assume that only 10% of the headgroup area in the pore walls comes from LPC, so that there is a molecular ratio of SPC:LPC of 9:1, with similar headgroup area for both SPC and LPC, which would still mean that LPC is significantly enriched in the (hypothetical) pores compared to the bulk ratio of 14:1. Nevertheless, we make use of R_{pores} to estimate a pore density and the percentage of the vesicle area covered by pores considering a dispersion of unilamellar vesicles (Table 2).

4 Conclusions

In this article, the effect of the presence of small amounts of lysophosphatidylcholine (18:1, LPC) on soybean phosphatidylcholine (SPC) liposomes has been studied using light scattering

and small-angle neutron scattering (SANS). We find that extrusion of liposomes with added LPC results in smaller liposomes which is probably a result of extruding bilayers of lower rigidity.[21,22] Most importantly, results of our model-free analysis of SANS curves suggest that the presence of water in the liposomes increases with added LPC as the fraction of incorporated water in the membrane rises to about 10–15% in dispersions with a higher LPC ratio. This could be assigned to the formation of LPC stabilized pores that allow for an increased water fraction to penetrate across the lipid bilayer, but, of course, could also arise from other structural changes of the bilayer. Accordingly, we estimate a pore size and density from said volume fraction for the different LPC ratios. However, if pores of the estimated sizes were present, they should be evidenced by other techniques such as electron microscopy, which to the best of our knowledge, is not the case. So, we assume that there either are no pores or if there should be pores in the membrane, the walls of these pores do not exclusively consist of LPC but can be enriched in LPC even though the addition of LPC promotes the incorporation of water in the membranes.

Furthermore, the difference in values of hydrodynamic radius (R_h), and water presence within the bilayer are modest for the different samples with added LPC at the different ratios (SPC : LPC 98 : 2, 96 : 4, 91 : 9). That is: R_h values vary between 54–56 nm and the volume fraction of incorporated water with respect to the lipid fraction between 15–20% v. In other words, rather small amounts of LPC affect the properties of the liposomes, but addition of more LPC does not have a significant further impact. It is possible for lysolipids to start forming micelles at the employed concentrations, in which case additional LPC would only continue to contribute to the micellar assembly.[11] Additional LPC molecules would apparently not stabilize further the transient pores. This could explain why $\phi_{D_2O}^{lipo}$ slightly decreases at higher SPC : LPC ratios.

Author contributions

F. A. designed and performed the experiments, analyzed and interpreted the data, and wrote the manuscript; I. H. helped with data interpretation, contributed to the writing of the manuscript, and dealt with project administration; M. G. conceptualized the work, contributed to the writing of the manuscript, and dealt with project administration; J. V. helped with conceptualization of the work, editing of the manuscript and project administration; N. M. performed the SANS measurements and data integration; All authors have read and agreed to the published version of the manuscript.

Data availability

The data supporting this article have been included as part of the ESI.† SANS data for this article is available at **https://doi. org/10.5286/ISIS.E.RB2210042**.

Conflicts of interest

There are no conflicts to declare.

Acknowledgements

Notes and references

1 D. Lasic and D. Papahadjopoulos, *Medical applications of liposomes*, Elsevier Science Bv, 1998.
2 G. Gregoriadis, *Nature*, 1977, **265**, 407–411.
3 M. Malmsten, *Soft Matter*, 2006, **2**, 760–769.
4 J. Ruiz, F. M. Goñi and A. Alonso, *Biochim. Biophys. Acta*, 1988, **937**, 127–134.
5 G. Nasr, H. Greige-Gerges, A. Elaissari and N. Khreich, *Int. J. Pharm.*, 2020, **580**, 119198.
6 F. Goñi and A. Alonso, *An. R. Acad. Nac. Farm.*, 2021, 53–96.
7 H. Heerklotz, *Q. Rev. Biophys.*, 2008, **41**, 205–264.
8 D. Lichtenberg, E. Opatowski and M. M. Kozlov, *Biochim. Biophys. Acta*, 2000, **1508**, 1–19.
9 R. E. Stafford, T. Fanni and E. A. Dennis, *Biochemistry*, 1989, **28**, 5113–5120.
10 V. A. Bjørnestad and R. Lund, *Langmuir*, 2023, **39**, 3914–3933.
11 H. Y. Fan, D. Das and H. Heerklotz, *Langmuir*, 2016, **32**, 11655–11663.
12 A. Pizzirusso, A. De Nicola, G. J. A. Sevink, A. Correa, M. Cascella, T. Kawakatsu, M. Rocco, Y. Zhao, M. Celino and G. Milano, *Phys. Chem. Chem. Phys.*, 2017, **19**, 29780–29794.
13 J. Israelachvili, S. Marčelja and R. Horn, *Q. Rev. Biophys.*, 1980, **13**(2), 121–200.
14 T. P. Sudbrack, N. L. Archilha, R. Itri and K. A. Riske, *J. Phys. Chem. B*, 2011, **115**, 269–277.
15 E. Karatekin, O. Sandre, H. Guitouni, N. Borghi, P.-H. Puech and F. Brochard-Wyart, *Biophys. J.*, 2003, **84**, 1734–1749.
16 D. Velluto, C. Gasbarri, G. Angelini and A. Fontana, *J. Phys. Chem. B*, 2011, **115**, 8130–8137.
17 J. Davidsen, O. G. Mouritsen and K. Jørgensen, *Biochim. Biophys. Acta, Biomembr.*, 2002, **1564**, 256–262.
18 T. Kitagawa, K. Inoue and S. Nojima, *J. Biochem.*, 1976, **79**, 1123–1133.
19 R. T. Hamilton and E. W. Kaler, *J. Phys. Chem.*, 1990, **94**, 2560–2566.
20 C. Van Echteld, B. De Kruijff, J. Mandersloot and J. De Gier, *Biochim. Biophys. Acta, Biomembr.*, 1981, **649**, 211–220.
21 T. J. McIntosh, S. Advani, R. E. Burton, D. V. Zhelev, D. Needham and S. A. Simon, *Biochemistry*, 1995, **34**, 8520–8532.
22 D. Otten, M. F. Brown and K. Beyer, *J. Phys. Chem. B*, 2000, **104**, 12119–12129.
23 J. R. Henriksen, T. L. Andresen, L. N. Feldborg, L. Duelund and J. H. Ipsen, *Biophys. J.*, 2010, **98**, 2199–2205.
24 R. S. Gracià, N. Bezlyepkina, R. L. Knorr, R. Lipowsky and R. Dimova, *Soft Matter*, 2010, **6**, 1472–1482.

25 V. Kumar, B. Malewicz and W. Baumann, *Biophys. J.*, 1989, **55**, 789–792.

26 J. H. Van Zanten and H. G. Monbouquette, *J. Colloid Interface Sci.*, 1991, **146**, 330–336.

27 J. F. Nagle, R. M. Venable, E. Maroclo-Kemmerling, S. Tristram-Nagle, P. E. Harper and R. W. Pastor, *J. Phys. Chem. B*, 2019, **123**, 2697–2709.

28 *Mantid: Manipulation and Analysis Toolkit for Instrument Data, Mantid Project*, 2013, DOI: **10.5286/SOFTWARE/MANTID.**

29 F. Alvarado Galindo, J. Venzmer, S. Prévost, I. Hoffmann and M. Gradzielski, *Colloids Surf., A*, 2024, **702**, 135014.

30 A. Alonso, R. Sáez, A. Villena and F. M. Goñi, *J. Membr. Biol.*, 1982, **67**, 55–62.

31 J. Mandersloot, F. Reman, L. Van Deenen and J. De Gier, *Biochim. Biophys. Acta, Biomembr.*, 1975, **382**, 22–26.

32 M. Müller, S. Mackeben and C. C. Müller-Goymann, *Int. J. Pharm.*, 2004, **274**, 139–148.

33 S. Y. Woo and H. Lee, *Phys. Chem. Chem. Phys.*, 2017, **19**, 21340–21349.

34 H. L. Scott, A. Skinkle, E. G. Kelley, M. N. Waxham, I. Levental and F. A. Heberle, *Biophys. J.*, 2019, **117**, 1381–1386.

35 W. Schärtl, *Light Scattering from Polymer Solutions and Nanoparticle Dispersions*, Springer Laboratory, 2007.

36 H. Frielinghaus, *Phys. Rev. E: Stat., Nonlinear, Soft Matter Phys.*, 2007, **76**, 051603.

37 M. Gradzielski, D. Langevin and B. Farago, *Phys. Rev. E: Stat. Phys., Plasmas, Fluids, Relat. Interdiscip. Top.*, 1996, **53**, 3900–3919.

38 J. Yoo and Q. Cui, *Biophys. J.*, 2009, **97**, 2267–2276.

39 P. Vinson, Y. Talmon and A. Walter, *Biophys. J.*, 1989, **56**, 669–681.

40 D. Lichtenberg, H. Ahyayauch and F. M. Goñi, *Biophys. J.*, 2013, **105**, 289–299.

41 O. A. Ogunsola, M. E. Kraeling, S. Zhong, D. J. Pochan, R. L. Bronaugh and S. R. Raghavan, *Soft Matter*, 2012, **8**, 10226–10232.

42 K. J. Seu, L. R. Cambrea, R. M. Everly and J. S. Hovis, *Biophys. J.*, 2006, **91**, 3727–3735.

43 N. D. Winter and G. C. Schatz, *J. Phys. Chem. B*, 2010, **114**, 5053–5060.

44 J. K. Mills and D. Needham, *Biochim. Biophys. Acta, Biomembr.*, 2005, **1716**, 77–96.

45 V. V. Kumar, *Proc. Natl. Acad. Sci. U. S. A.*, 1991, **88**, 444–448.

46 C. Faure, L. Bonakdar and E. J. Dufourc, *FEBS Lett.*, 1997, **405**, 263–266.

47 O. Tirosh, Y. Barenholz, J. Katzhendler and A. Priev, *Biophys. J.*, 1998, **74**, 1371–1379.

48 P. Balgavý, M. Dubničková, N. Kučerka, M. A. Kiselev, S. P. Yaradaikin and D. Uhríková, *Biochim. Biophys. Acta, Biomembr.*, 2001, **1512**, 40–52.

49 J. F. Nagle and S. Tristram-Nagle, *Biochim. Biophys. Acta, Biomembr.*, 2000, **1469**, 159–195.